IEEE Access
Multidisciplinary : Rapid Review : Open Access Journal

Received June 22, 2019, accepted July 4, 2019, date of publication July 8, 2019, date of current version August 2, 2019.

Digital Object Identifier 10.1109/ACCESS.2019.2927231

An Improved 4H-SiC Trench MOS Barrier Schottky Diode With Lower On-Resistance

FEI CAO[1], MENG-TIAN BAO[1], XUE WU[2], WEN-JU WANG[1], CHENG-HAO YU[1], AND YING WANG[1], (Senior Member, IEEE)

[1]The Key Laboratory of RF Circuits and Systems, Ministry of Education, Hangzhou Dianzi University, Hangzhou 310018, China
[2]National Key Laboratory of Analog Integrated Circuits, Chongqin 400060, China

Corresponding authors: Fei Cao (caofei@hdu.edu.cn) and Cheng-hao Yu (yuchenghao@hdu.edu.cn)

This work was supported in part by the National Natural Science Foundation of China under Grant 61774052, and in part by the Science and Technology on Analog Integrated Circuit Laboratory under Grant 6142802180507.

ABSTRACT An improved 4H-SiC trench MOS barrier Schottky (TMBS) structure that can significantly reduce the specific on-resistance ($R_{on,sp}$) is proposed in this paper. Compared with the conventional TMBS structure, an N-type region is added around the P+ shielding region and along the trench sidewall in the proposed structure, and the doping concentration is higher than that of the drift region. The JFET resistance, and spread resistance can both be reduced significantly during the forward bias to produce a much lower $R_{on,sp}$, which have been verified through the numeric simulations and modeling analysis. The critical parameters (N-type region width and its doping concentration) of the proposed structure are mainly optimized by the ATLAS simulation tool. As a result, the breakdown voltage and leakage current of the improved structure remain basically unchanged compared with the conventional TMBS. However, the $R_{on,sp}$ and FoM ($BV^2/R_{on,sp}$) can be effectively improved by 41.9% and 70.9%, respectively.

INDEX TERMS 4H-SiC, TMBS, JFET, analytical model, specific ON-resistance, electric field.

I. INTRODUCTION

Silicon carbide (SiC) has many excellent characteristics that makes it suitable for high temperature, high voltage, and high power applications [1], [2]. Compared with Si-based PiN diode, 4H-SiC Schottky barrier diode (SBD) has a relatively simple manufacturing process and behaves lower conduction voltage and faster switching speed [3], [4]. However, its reverse leakage current degenerates rapidly when Schottky surface electric field is high enough that a tunneling effect occurs [5]. In order to avoid tunneling current and maintain low conduction voltage, junction barrier Schottky (JBS) diode is proposed [6], [7]. As the junction depth of P+ region is limited by ion implantation energy, there is a tradeoff between on-resistance (R_{on}) and breakdown voltage (BV) in JBS devices. The trench JBS (TJBS) devices have solved this problem effectively by making a larger design window that enables good reverse blocking and forward conduction capabilities at the same time [8]–[10]. The 4H-SiC TMBS devices are of interest because they don't need costly implantations that have been developed by some structural optimizations and process improvements [11], [12]. One of the them is that, by adding a P+ shielding region below the trench bottom, the electric field distributions within the oxide layer and Schottky interface can be significantly reduced. However, the P+ shielding region also brings the JFET resistance at the same time, which increases the R_{on} of a device. For solving this problem, we further add an N-type region around the P+ shielding region that the $R_{on,sp}$ and FoM can be both effectively improved [13]. In order to enhance the electric characteristics of a device further, an improved 4H-SiC TMBS structure has been proposed in this paper. By introducing an additional sidewall layer in the structure, a lower $R_{on,sp}$ and larger FoM can both be realized compared with that in [13].

The associate editor coordinating the review of this manuscript and approving it for publication was Jiajie Fan.

II. FABRICATION PROCEDURE AND PARAMETERS

The schematic cross-sectional views of improved 4H-SiC TMBS and conventional 4H-SiC TMBS are presented in Fig. 1. By adding an N-type region around the P+ shielding region and along the trench sidewall, the depletion width of

 This work is licensed under a Creative Commons Attribution 4.0 License. For more information, see http://creativecommons.org/licenses/by/4.0/

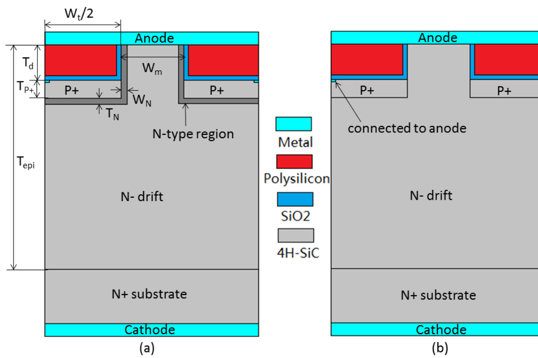

FIGURE 1. The schematic cross-sectional views of the improved 4H-SiC TMBS (a) and conventional 4H-SiC TMBS (b).

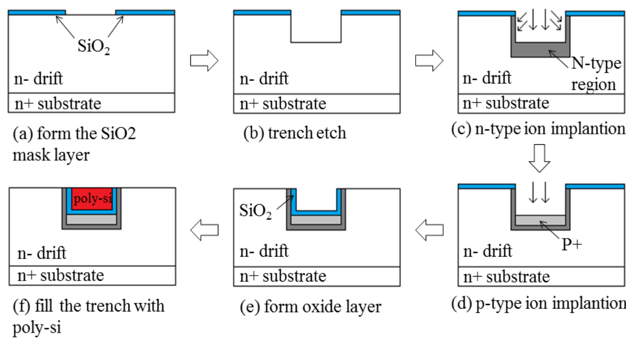

FIGURE 2. Main fabrication steps of the improved 4H-SiC TMBS structure.

PN junction can be reduced that promoting the current expansion within the drift region, as a result, the JFET resistance and spread resistance are significantly improved.

The main fabrication steps of improved structure are given in Fig. 2. Firstly, the doping concentration and thickness of drift region are given. After the SiO_2 masking layer is made (Fig. 2(a)), the trench using the ICP method can be etched as shown in Fig. 2(b) [14]. Then, an N-type ion implantation is implemented to form the bottom and sidewall of trench (Fig. 2(c)). Afterwards, a P-type ion implantation that forms P+ shielding region can be seen in Fig. 2(d). Next, the oxide layer is formed by the thermal oxidation and PECVD method (Fig. 2(d)) [15]. Finally, the trench is filled with polysilicon as shown in Fig. 2(f).

III. SIMULATION RESULTS AND DISCUSSION

In this paper, we use the Silvaco numerical simulation tool to optimize the forward and reverse characteristics of devices. Firstly, the basic physical models used in simulations include the Fermi–Dirac statistics and bandgap narrowing models which account for the carrier statistic. The mobility models consider the dependencies of carrier concentration, temperature, and electric field. In addition, Shockley–Read–Hall (SRH) and Auger recombination models should be employed in this paper. Selberherr's impact ionization model is introduced to calculate the ionization rate that has a great influence on the breakdown. Incomplete ionization and electro-thermal models are also considered because high temperature and large current density conditions are referred in the forward characteristic [16]. The specific parameters for the optimal device structure are listed in TABLE 1.

TABLE 1. Optimal devices parameters for the simulations.

Parameter	Improved TMBS	Conventional TMBS
Width of trench (W_t)	4.0 μm	4.0 μm
Width of Mesa (W_M)	2.0 μm	2.0 μm
Thickness of epilayer (T_{epi})	11 μm	11 μm
Epilayer Doping (N_{epi})	5×10^{15} cm^{-3}	5×10^{15} cm^{-3}
Etch depth of trench (T_d)	1.0 μm	1.0 μm
Thickness of oxide (T_{ox})	0.1 μm	0.1 μm
P+ junction depth (T_{p+})	0.4 μm	0.4 μm
Width of N-type region (W_N)	0.1 μm	--
Thickness of N-type region (T_N)	0.1 μm	--
N-type region Doping (N_N)	1×10^{17} cm^{-3}	--
Schottky barrier height (Φ_{Bn})	1.2 eV	1.2 eV

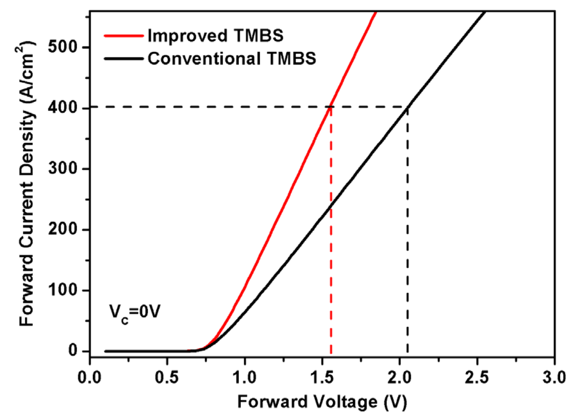

FIGURE 3. Forward *I-V* characteristics of the improved TMBS and conventional TMBS.

A. FORWARD CHARACTERISTICS

The forward I-V characteristics of improved TMBS and conventional TMBS (a positive voltage applied to the anode) are shown in Fig. 3. It is obvious that the slope of forward I-V curve which determines $R_{on,sp}$ for improved structure is much larger than that for conventional structure. According to the dash line which indicates the forward voltage (V_F) at a forward current density (J_F) of 400 A/cm^2, the V_F of improved TMBS and conventional TMBS are 1.6 V and 2.1 V, respectively. As a result, the conduction loss for improved TMBS can be reduced.

Fig. 4(a) and (b) demonstrate the forward current contour of two structures at $J_F = 400$ A/cm^2, respectively. We can see that the current path of improved structure is wider because of a narrower PN junction depletion width. So, the R_{on} of improved TMBS can be significantly reduced as Fig. 3 shows. In order to prove the validity of our simulation results further, we have developed the analysis model of $R_{on,sp}$ that will be discussed in detail as follows.

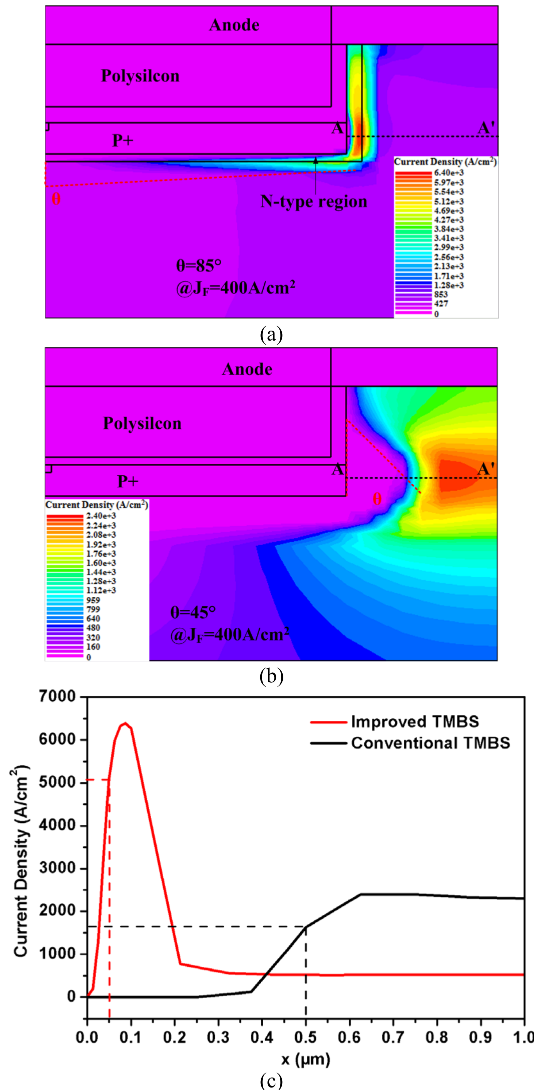

FIGURE 4. Forward current density contours of (a) improved TMBS and (b) conventional TMBS at J_F = 400A/cm^2 and (c) the current density along with the AA′ in (a).

Considering that the trench occupies a part of the Schottky contact area, the Schottky contact current density (J_{FS}) is given by

$$J_{FS} = \frac{P}{S} J_F \tag{1}$$

where P represents the pitch width, S denotes the Schottky contact width as shown in Fig. 5. So, the Schottky contact voltage (V_{FS}) can be expressed by the thermionic emission model:

$$V_{FS} = \Phi_{Bn} + \frac{kT}{q} \ln\left(\frac{P}{S}\frac{J_{FS}}{AT^2}\right) \tag{2}$$

where Φ_{Bn} is the Schottky barrier height, k is the Boltzmann constant, and the T is the thermodynamic temperature.

Besides the V_{FS}, the other component of V_F is caused by the $R_{on,sp}$ in a conventional TMBS:

$$R_{on,sp} = R_{ch,sp} + R_{JFET,sp} + R_{spread,sp} + R_{D,sp} + R_{sub,sp} + R_{C,sp} \tag{3}$$

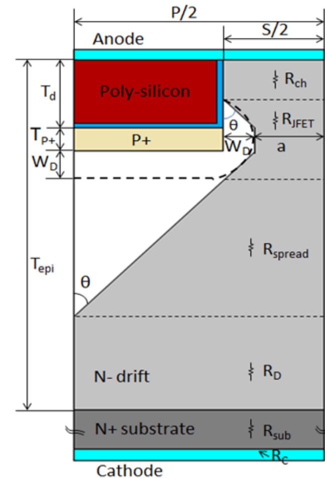

FIGURE 5. Current path analysis model in conventional TMBS during forward conduction.

where the specific substrate resistance ($R_{sub,sp}$) and specific cathode contact resistance ($R_{C,sp}$) can be neglected compared with the other four main parts: specific channel resistance ($R_{ch,sp}$), specific JFET resistance ($R_{JFET,sp}$), specific spread resistance ($R_{spread,sp}$) and specific drift resistance ($R_{D,sp}$). So, $R_{on,sp}$ can be simplified by:

$$R_{on,sp} = R_{ch,sp} + R_{JFET,sp} + R_{spread,sp} + R_{D,sp} \tag{4}$$

The formulas of $R_{ch,sp}$, $R_{JFET,sp}$, $R_{spread,sp}$ and $R_{D,sp}$ can be acquired by numerical integration as follows:

$$R_{ch,sp} = \left(\frac{P}{S}\right) \cdot \rho_D \cdot (T_d - \frac{W_D}{\tan(\theta)}) \tag{5}$$

$$R_{JFET,sp} = \frac{P \cdot \rho_D}{\tan(\theta)} \cdot \ln\left(1 + \frac{W_D}{a}\right) + \frac{P}{2a} \cdot \rho_D \cdot T_{P+} \tag{6}$$

$$R_{spread,sp} = \frac{P \cdot \rho_D}{2 \cdot \tan(\theta)} \ln\left(\frac{P}{2a}\right) \tag{7}$$

$$R_{D,sp} = \rho_D \cdot (T_{epi} - T_d - T_{P+} - \frac{P/2 - a}{\tan(\theta)}) \tag{8}$$

Note that the P+ shielding region brings the PN junction depletion region, the $R_{JFET,sp}$ must be considered [17], [18]. The PN junction depletion width (W_D) can be expressed by equation (9) that varies with V_F.

$$W_D = \sqrt{\frac{2\varepsilon_s(V_{bi} - V_F)}{qN_D}} \tag{9}$$

The resistivity of drift region [19] can be expressed by:

$$\rho_D = \frac{1}{q\mu_n N_D} \tag{10}$$

In addition, the electrical behavior of 4H-SiC TMBS depends strongly on the operating temperature of a device, the model for temperature and concentration dependences of electron mobility [20]–[22] is given as follows:

$$\mu_n = 40 + \frac{900}{1 + \left(\frac{N_D}{4.5 \times 10^{17}}\right)^{0.45}} \cdot \left(\frac{T}{300K}\right)^{-3} \tag{11}$$

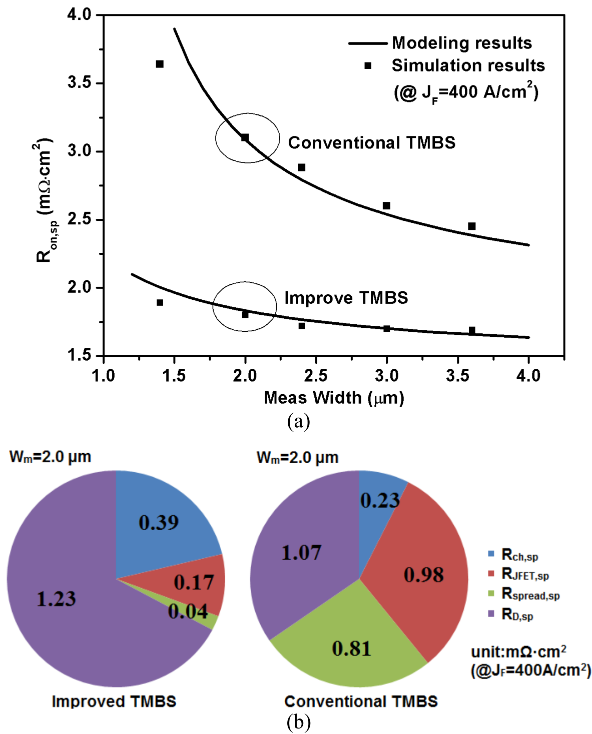

FIGURE 6. Comparison of (a) the calculated specific on-resistance using our model with the simulated results (b) the specific on-resistance of each part for both improved and conventional structures.

As shown in Fig. 5, θ is a very important parameter on calculating $R_{on,sp}$ of a device. The value of θ is equal to 45° for conventional TMBS as shown in Fig. 4(b). However, the conventional analytical model needs to be modified because the current spread more significantly in the vicinity of N-type region as shown in Fig. 4(a). Therefore, a larger θ (85°) should be introduced to give a correct result. What's more, the W_D of improved structure decreases from 0.5 μm (conventional TMBS) to 0.05 μm as shown in Fig. 4(c) due to a higher N_N according to equation (9). As a consequence, the $R_{JFET,sp}$ and $R_{spread,sp}$ of improved TMBS can be both reduced significantly according to equation (6) and (7) to generate a much lower $R_{on,sp}$.

For certifying the correctness of our analytical model, the calculated results and simulated results of two structures are shown Fig. 6(a). We can see that the analytical model is well consistent with our simulation results, and the $R_{on,sp}$ of improved TMBS is much lower than that of conventional one at different mesa width. Moreover, we can see that the $R_{JFET,sp}$ and $R_{spread,sp}$ of improved structure both decreases a lot as shown in Fig. 6(b) which has been explained through the forward current density contours in Fig. 4.

B. REVERSE CHARACTERISTICS

Fig. 7 demonstrates the reverse I-V characteristic of two structures with a negative voltage applied to the anode. The breakdown voltages of improved TMBS and conventional TMBS are 1895 V and 1905 V, respectively, which are almost the same. We know that the Schottky interface electric field (E_S) degenerates seriously by increasing the mesa width [18]. Therefore, the E_S must be suppressed to avoid tunneling effect that the leakage current density can be limited to an acceptable level. To achieve that, the barrier width needs to be larger 12 nm. Based on this, the maximal E_S can be calculated as 1.0 MV/cm with $\Phi_{Bn} = 1.2$ eV [5]. The insert figure shows that the E_S of improved TMBS is larger than that of conventional one because of a narrower PN junction depletion width, but the E_S remains lower than 1.0 MV/cm without producing a tunneling current. As a result, the reverse leakage current densities (thermionic emission leakage current) are almost the same in the two structures [5], [8].

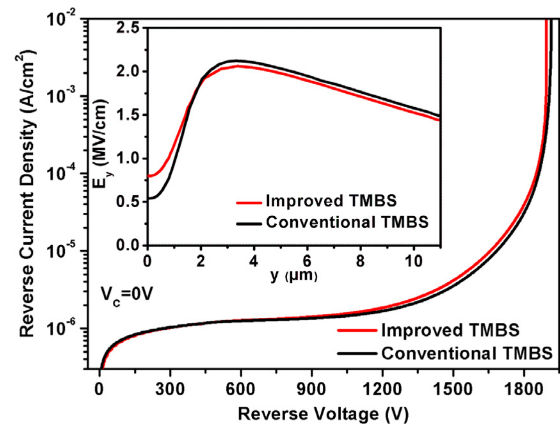

FIGURE 7. The reverse *I-V* characteristics and electric field distributions across the meas of the improved TMBS and conventional TMBS.

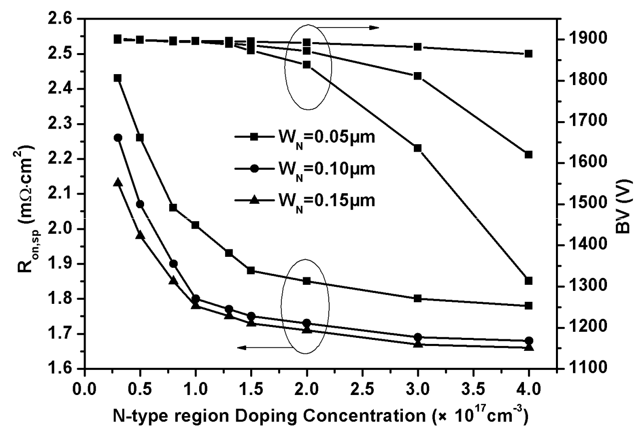

FIGURE 8. The simulation results for specific on-resistance and breakdown voltage of the improved TMBS.

C. PARAMETER OPTIMIZATION

In Fig. 8, we give the parameter optimization analysis of improved structure with different N_N and W_N. Firstly, we can see that $R_{on,sp}$ is relatively large when N_N is small for etch curve (less than 1.5×10^{17} cm^{-3}), and decreases obviously as the N_N increases. This is because the depletion width is reduced with the increase in N_N, the $R_{ch,sp}$ and $R_{JFET,sp}$ can decrease quickly. However, the $R_{on,sp}$ gradually reaches saturation when N_N is larger than 2.0×10^{17} cm^{-3}. The $R_{on,sp}$ also decreases from $W_N = 0.05$ to 0.15 μm, because the

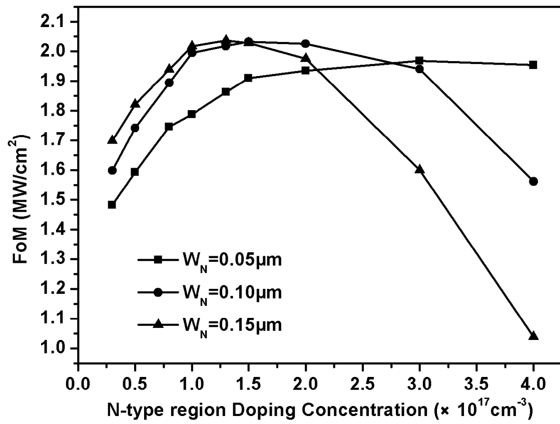

FIGURE 9. The simulation results of FoM for the improved TMBS.

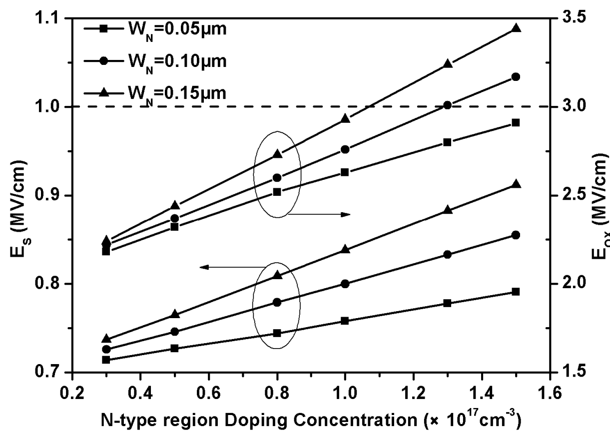

FIGURE 10. The simulation results for maximum electric field strength of schottky interface and oxide under breakdown voltage of the improved TMBS.

depletion width can be enlarged by increasing W_N. But the $R_{on,sp}$ is hardly reduced when W_N is larger than 0.10 μm. In contrast, the breakdown voltage (BV) remains almost the same when N_N is less than 1.5×10^{17} cm^{-3}. But the BV decreases significantly if N_N exceeds 2.0×10^{17} cm^{-3}. What's more, the BV with a wider W_N degenerates rapidly because the shielding effect for the electric field will get much weaker.

Fig. 9 demonstrates the simulation results of FoM based on the $R_{on,sp}$ and BV as shown in Fig. 8. Initially, we can see that the FoM increases fast with increasing of N_N because the $R_{on,sp}$ decreases quickly while the BV decreases slightly. Afterwards, the FoM tends to reach a maximum value with a further increase in N_N. Then, the FoM starts to decrease as the BV degenerates significantly while the $R_{on,sp}$ is hardly changed. Besides the N_N, the W_N also has a great influence on the FoM that BV decreases more rapidly with a wider W_N because the electric field shielding effect gets worse.

To investigate the operating stability of improved structure, we present the maximum electric field of E_S and oxide layer (E_{OX}) at different N_N and W_N conditions in Fig. 10. We also set $E_S = 1.0$ MV/cm and $E_{OX} = 3.0$ MV/cm as the critical conditions (dotted line) that the device must be avoid [5]. From Fig. 9 we can see that the FoM improves significantly with W_N increasing from 0.05 to 0.1 μm if N_N is below 2.0×10^{17} cm^{-3}, but increases a little if W_N increases to 0.15 μm. At the same time, the E_S and E_{OX} both increase obviously, thus, setting W_N to 0.1 μm can be suitable to give an optimal result. On that basis, we further find that E_S can be smaller than the ultimate value when N_N changes from 0.3×10^{17} to 1.5×10^{17} cm^{-3}. What's worse, the E_{OX} exceeds the critical value if N_N increases to 1.3×10^{17}cm^{-3}. Therefore, $N_N = 1.0 \times 10^{17}$ cm^{-3} is more appropriate to give a trade-off between the operating stability and FoM. As a result, we set W_N to 0.1 μm and N_N to 1.0×10^{17}cm^{-3} as an optimal condition in this paper.

TABLE 2. Performance comparison.

Device types	BV (V)	$R_{on,sp}$ (mΩ·cm²)	FoM (MW/cm²)
Improved TMBS	1895	1.80	2.00
Conventional TMBS	1905	3.10	1.17
Optimized p+ shielding TMBS [13]	1908	1.98	1.84

Table 2 summarizes the optimal results for the BV, $R_{on,sp}$, and FoM for several devices including the improved TMBS, conventional TMBS and our previous-proposed TMBS. As a consequence, the improved TMBS can present the best FoM performance that increases by 70.9% and 8.7% compared with the conventional one and the structure in reference [13].

IV. CONCLUSION

In this paper, an improved TMBS structure with a lower specific on-resistance achieved by adding the N-type region is proposed. The analytical models of both conventional and improved structures under forward bias are developed, and the key parameters (N_N and W_N) are discussed and optimized by using ATLAS simulation tool. The simulation results illustrate that the breakdown voltage of improved TMBS remains basically unchanged compared with conventional one. However, the specific on-resistance of improved TMBS decreases by 41.9% and the FoM increases by 70.9% compared to the conventional TMBS with the same device dimensions.

REFERENCES

[1] J. Wu, N. Ren, H. Wang, and K. Sheng, "1.2 kV 4H-SiC merged PiN Schottky diode with improved surge current capability," *IEEE J. Emerg. Sel. Topics Power Electron.*, to be published. doi: 10.1109/JESTPE.2019.2921970.

[2] H. Bartolf, A. Mihaila, L. Knoll, V. K. Sundaramoorthy, R. A. Minamisawa, and E. Bianda, "JBS power-rectifiers for 1.7 kV applications with conduction properties close to pure Schottky-design," in *Proc. 17th Eur. Conf. Power Electron. Appl. (EPE ECCE-Eur.)*, Sep. 2015, 1–10. doi: 10.1109/EPE.2015.7311684.

[3] X. Huang, G. Wang, M.-C. Lee, and A. Q. Huang, "Reliability of 4H-SiC SBD/JBS diodes under repetitive surge current stress," in *Proc. IEEE Energy Convers. Congr. Expo. (ECCE)*, Sep. 2012, pp. 2245–2248. doi: 10.1109/ECCE.2012.6342436.

[4] R. Singh, J. A. Cooper, M. R. Melloch, T. P. Chow, and J. W. Palmour, "SiC power Schottky and PiN diodes," *IEEE Trans. Electron Devices*, vol. 49, no. 4, pp. 665–672, Apr. 2002.

[5] N. Ren, J. Wang, and K. Sheng, "Design and experimental study of 4H-SiC trenched junction barrier Schottky diodes," *IEEE Trans. Electron Devices*, vol. 61, no. 7, pp. 2459–2465, Jul. 2014.

[6] R. Singh, S. Ryu, J. W. Palmour, A. R. Hefner, and J. Lai, "1500 V, 4 amp 4H-Sic JBS diodes," in *Proc. 12th Int. Symp. Power Semiconductor Devices ICs*, May 2000, pp. 101–104.

[7] J. H. Zhao, P. Alexandrov, L. Fursin, Z. C. Feng, and M. Weiner, "High performance 1500 V 4H-SiC junction barrier Schottky diodes," *Electron. Lett.*, vol. 38, no. 22, pp. 1389–1390, Oct. 2002.

[8] K. Konishi, N. Kameshiro, N. Yokoyama, A. Shima, and Y. Shimamoto, "Effect of trench structure on reverse characteristics of 4H-SiC junction barrier Schottky diodes," *Jpn. J. Appl. Phys.*, vol. 56, no. 12, 2017, Art. no. 121301.

[9] Q. C. J. Zhang, J. Duc, V. Mieczkowski, B. Hull, S. Allen, and J. Palmour, "4H-SiC trench Schottky diodes for next generation products," *Mater. Sci. Forum*, vols. 740–742, pp. 781–784, Jan. 2013.

[10] T. Nakamura, Y. Nakano, M. Aketa, R. Nakamura, S. Mitani, H. Sakairi, and Y. Yokotsuji, "High performance SiC trench devices with ultra-low ron," in *IEDM Tech. Dig.*, Washington, DC, USA, Dec. 2011, pp. 26.5.1–26.5.3.

[11] K. Byung-Soo and K. Kwang-Soo, "A 4H-SiC trench MOS barrier Schottky (TMBS) rectifier using the trapezoid mesa and the upper half of sidewall," *J. IKEEE*, vol. 17, no. 4, pp. 428–433, Dec. 2013.

[12] C.-Y. Lee, C.-T. Yen, K.-W. Chu, Y.-S. Chen, C.-C. Hung, L.-S. Lee, T.-M. Yang, C.-S. Chuang, C.-C. Huang, and M.-J. Tsai, "A novel 4H-SiC trench MOS barrier Schottky rectifier fabricated by a two-mask process," in *Proc. 25th Int. Symp. Power Semiconductor Devices IC's*, Kanazawa, Japan, May 2013, pp. 171–174.

[13] Y. Wang, W.-J. Wang, C.-H. Yu, Y.-F. Huang, Y.-L. Sun, and J.-X. Tang, "An optimized 4H-SiC trench MOS barrier Schottky (TMBS) Rectifier," *IEEE J. Electron Devices Soc.*, vol. 6, pp. 1154–1158, 2018.

[14] Y. Kawada, T. Tawara, S.-I. Nakamura, T. Tamori, and N. Iwamuro, "Shape control and roughness reduction of sic trenches by high-temperature annealing," *Jpn. J. Appl. Phys.*, vol. 48, no. 11R, 2009, Art. no. 116508.

[15] C. T. Banzhaf, M. Grieb, A. Trautmann, A. J. Bauer, and L. Frey, "Characterization of diverse gate oxides on 4H-SiC 3D trench-MOS structures," *Mater. Sci. Forum*, vols. 740–742, pp. 691–694, Jan. 2013.

[16] *ATLAS User's Manual: Device Simulation Software*, Silvaco Int., Santa Clara, CA, USA, 2016.

[17] B. J. Baliga, *Advanced Power Rectifier Concepts*. Boston, MA, USA: Springer, 2009.

[18] L. Zhu and T. P. Chow, "Analytical modeling of high-voltage 4H-SiC junction barrier Schottky (JBS) rectifiers," *IEEE Trans. Electron Devices*, vol. 55, no. 8, pp. 1857–1863, Aug. 2008.

[19] B. J. Baliga, *Fundamentals of Power Semiconductor Devices*. New York, NY, USA: Springer, 2008.

[20] M. Roschke and F. Schwierz, "Electron mobility models for 4H, 6H, and 3C SiC," *IEEE Trans. Electron Devices*, vol. 48, no. 7, pp. 1442–1447, Jul. 2001. doi: 10.1109/16.930664.

[21] K. Chatty, T. P. Chow, R. J. Gutmann, E. Arnold, and D. Alok, "Accumulation-layer electron mobility in n-channel 4H-SiC MOSFETs," *IEEE Electron Device Lett.*, vol. 22, no. 5, pp. 212–214, May 2001.

[22] T. Kobayashi and T. Kimoto, "Carbon ejection from a SiO_2/SiC(0001) interface by annealing in high-purity Ar," *Appl. Phys. Lett.*, vol. 111, no. 6, 2017, Art. no. 062101.

FEI CAO received the B.S. degree in electronic science and technology and the M.S. degree in microelectronics and solid state electronics from Liaoning University, China, in 2004 and 2009, respectively, and the Ph.D. degree in material science from the Harbin Institute of Technology, China, in 2016.

She is currently with the Hangzhou Dianzi University as a Lecturer. For many years, she has been engaged in the research of semiconductor device structure design and metallization technology. She has experience in semiconductor device fabrication and related performance characterization and analysis, and has accumulated a certain theoretical and experimental basis in semiconductor device metallization and interconnection technology.

MENG-TIAN BAO received the B.S. degree in microelectronics, the M.S. degree in electronic and communication engineering, and the Ph.D. degree in information and communication engineering from Harbin Engineering University, China, in 2008, 2012, and 2019, respectively.

She is currently with the Hangzhou Dianzi University as a Lecturer. For many years, she has been engaged in the research of semiconductor device structure design and metallization technology. Her current research interests include SiC power devices design and the irradiation effect analysis.

XUE WU , photographs and biographies not available at the time of publication.

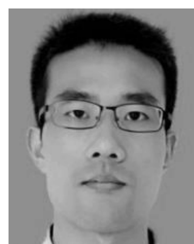

WEN-JU WANG received the B.S. degree in communication engineering from Henan Normal University, China, in 2015, and the M.S. degree in electronic and communication engineering from Hangzhou Dianzi University, China, in 2019.

He had interested in researching new structure and key technologies of power transistor with the third generation wide-gap semiconductor materials, and optimizing device structure and performance by theoretical analysis and simulation.

CHENG-HAO YU received the B.S. degree in microelectronics and the Ph.D. degree in information and communication engineering from Harbin Engineering University, China, in 2007 and 2016, respectively.

In 2016, he joined the Key Laboratory of RF Circuits and Systems, Ministry of Education, Hangzhou Dianzi University, Hangzhou, China, where he is currently a Lecturer. He is currently researching on the advanced power semiconductor devices and space radiation effects.

YING WANG (SM'17) received the B.S. degree in microelectronics and the M.S. degree in microelectronics and solid state electronics from Liaoning University, China, in 1999 and 2002, respectively, and the Ph.D. degree in electronic science and technology from Xi'an Jiaotong University, China, in 2005.

From 2005 to 2016, he was with the Harbin Engineering University, China, where he became a Professor, in 2009. He is currently with the Key Laboratory of RF Circuits and Systems, Ministry of Education, Hangzhou Dianzi University, Hangzhou, China. He has rich experience in the research of microelectronic devices and integration technology, power semiconductor devices, and micro-sensor design. He has over 70 publications and is the holder of 22 patents. His current research and development interests include the advanced SiC/GaN power semiconductor devices design and simulation, the space radiation effects, and enhanced method analysis.